Effect of Mg-Preflow for p-AlGaN Electron Blocking Layer on the Electroluminescence of Green LEDs with V-Shaped Pits *

Ai-Xing Li(李爱星), Chun-Lan Mo(莫春兰)**, Jian-Li Zhang(张建立), Xiao-Lan Wang(王小兰), Xiao-Ming Wu(吴小明), Guang-Xu Wang(王光绪), Jun-Lin Liu(刘军林), Feng-Yi Jiang(江风益)

National Institute of LED on Silicon Substrate, Nanchang University, Nanchang 330047

(Received 17 November 2017)

InGaN-based green light-emitting diodes (LEDs) with and without Mg-preflow before the growth of p-AlGaN electron blocking layer (EBL) are investigated experimentally. A higher Mg doping concentration is achieved in the EBL after Mg-preflow treatment, effectively alleviating the commonly observed efficiency collapse and electrons overflowing at cryogenic temperatures. However, unexpected decline in quantum efficiency is observed after Mg-preflow treatment at room temperature. Our conclusions are drawn such that the efficiency decline is probably the result of different emission positions. Higher Mg doping concentration in the EBL after Mg-preflow treatment will make it easier for a hole to be injected into multiple quantum wells with emission closer to p-GaN side through the c-plane rather than the V-shape pits, which is not favorable to luminous efficiency due to the preferred occurrence of accumulated strain relaxation and structural defects in upper QWs closer to p-GaN. Within this framework, apparently disparate experimental observations regarding electroluminescence properties, in this work, are well reconciled.

PACS: 73.61.Ey, 78.60.Fi, 73.21.Fg, 61.72.Ff DOI: 10.1088/0256-307X/35/2/027301

A growing interest has been evoked in the direct wide-bandgap gallium nitride (GaN)-based light-emitting diodes (LEDs), which are widely used in solid-state lighting and display fields.[1] However, high luminous efficiency of GaN-based LEDs can be only delivered at low current density, by virtue of efficiency droop at large current density, especially for the green LEDs.[2] Moreover, the issues on hole transportation have not been solved well so far, such as nonuniform hole distribution in the multiple quantum wells (MQWs) and the low injection efficiency, which are claimed to be important factors for efficiency droop.[3] Consequently, it is vital to address these issues for the further improvement in luminous efficiency. Recently, to improve the performance of InGaN/GaN LEDs, tremendous efforts have been devoted to promoting the hole transportation, mainly including optimizing epitaxial structures and p-type doping conditions. The p-InGaN hole-reservoir layers have been inserted in electron blocking layer (EBL) to reduce potential height for hole injection.[4] A p^+-GaN/InGaN/n^+-GaN polarization tunnel junction has also been integrated into the InGaN/GaN LED architecture to increase the probability for hole tunneling into MQWs.[5] Furthermore, the Mg-doping position ranging from the EBL to the MQWs has been explored and investigated systematically to reveal the underlying mechanism of p-type doping improvement.[6] Despite various reports on the improvement in hole transportation, it is still far from perfect and worthy of further investigation.

The p-type doping in the AlGaN EBL is essential since an undoped AlGaN EBL significantly impedes the holes transport into MQWs. Hence, we will focus on the effects of p-type doping in the p-AlGaN EBL on the photoelectrical property of InGaN/GaN LEDs. In this study, based on the InGaN-based green LEDs with V-shape pits (V-pits), two samples with and without Mg-preflow in the p-AlGaN EBL are grown on Si substrates and were investigated by secondary ion mass spectroscopy (SIMS) and electroluminescence (EL). Unexpected results are observed after Mg-preflow treatment at room temperature. Apparently disparate experimental observations regarding EL properties, in this work, are well reconciled.

Two samples taken in our experiment were grown on 1.2 mm × 1.2 mm patterned 2-inch silicon (111) substrates by a homemade metal organic chemical vapor deposition (MOCVD) system. For comparison, the epitaxial structures were identical, and schematically shown in Fig. 1. Mg-preflow treatment was carried out through a pre-flowing Cp_2Mg source (Mg precursor) into the reactor before the growth of p-AlGaN EBL. The samples without and with Mg-preflow were denoted as samples A and B, respectively, and the total Mg-preflow flow rate was 45 sccm (standard cubic centimeter per minute) in sample B. Both the samples were fabricated into vertical structure LED

*Supported by the National Key R&D Program of China under Grant Nos 2016YFB0400600 and 2016YFB0400601, the State Key Program of the National Natural Science of China under Grant No 61334001, the Key R&D Program of Jiangxi Province under Grant No 20165ABC28007, the Natural Science Foundation of Jiangxi Province under Grant No 20151BAB207053, and the National Natural Science Foundation of China under Grant No 21405076.

**Corresponding author. Email: mclan@ncu.edu.cn

© 2018 Chinese Physical Society and IOP Publishing Ltd

chips with the n-face surface up and roughened, and the effective area of the chip was 1 mm^2. The detailed epitaxial growth condition and chip fabrication process have been reported.[7,8] The SIMS data has been obtained using a CAMECA IMS 7f instrument. The dependences of EL on the temperature and current injection density have also been undertaken on the test system consisting of an integrating sphere and the CAS140CT spectrometer made by Instrument Systems, the temperature-controlling unit made by MMR Technologies, Inc., and the 2635 A Sourcemeter made by Keithley Instruments, Inc. The room-temperature dominant wavelengths of the two samples at typical forward current density of 20 A/cm^2 were around 525 nm.

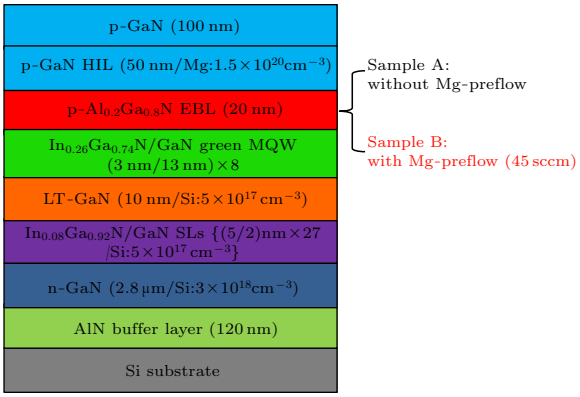

Fig. 1. Schematic epitaxial structure of the two samples with different growth processes of p-AlGaN EBL.

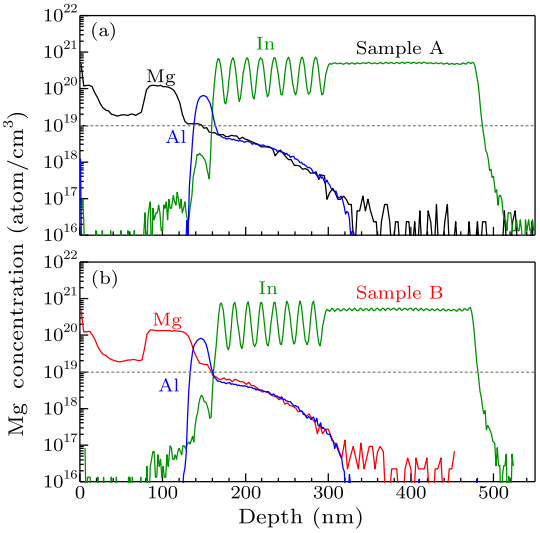

Fig. 2. Mg, Al, In profiles of samples A and B obtained by SIMS. The EBLs of samples A and B are obtained without or with Mg-preflow, respectively.

The atomic depth profiles of Mg, Al and In for samples A and B, plotted with the zero of the depth scale (depth=0) set to coincide with the position of the p-GaN surface, are shown in Figs. 2(a) and 2(b). The Al and In profiles are almost identical for the two samples, indicating that the thickness and composition of the p-AlGaN EBL and the MQWs are the same as intended. The higher Mg doping concentration is obtained in the whole p-AlGaN EBL of sample B compared with that of sample A, which can be ascribed to the difference of actual Cp_2Mg flow rate for deposition. When the Cp_2Mg is piped from the bubbler to the reactor, it is likely to stick to the pipes and reactor wall, which is known as memory effect.[9] The Mg-preflow just before the growth of p-AlGaN EBL makes the pipes and reactor covered with a certain amount of Cp_2Mg in advance. Thus for sample B, there will be more Cp_2Mg during the growth of p-AlGaN EBL participating in the deposition of p-AlGaN after the absorption by pipes and reactor surfaces, leading to higher Mg doping concentration in EBL. In addition, the Mg and Al detected in the MQWs of both the samples may be from the p-GaN and p-AlGaN in the V-pits.[10]

Figure 3(a) shows the EQE of samples A and B as a function of forward current density at room temperature (300 K). EQE of both the samples peaks at a certain current density (about 6 A/cm^2) and then deteriorates rapidly at higher injection current. The EQE ratio of sample A to sample B as a function of forward current density is plotted in the inset. Sample B shows lower EQE than sample A within the current density range of interest, but the disparity in EQE for both the samples reduces gradually as the current density rises. However, an unexpected result is found in Fig. 3(b) that sample B shows a higher normalized EQE at 100 K. As shown in Fig. 3(c), both the samples exhibit a spectral blueshift of peak wavelength (PW) at 300 K as the current density increases, and sample B shows an increased spectral blueshift of 25.9 nm compared with a spectral blueshift of 20.3 nm for sample A with the current density increasing from 0.07 A/cm^2 to 20 A/cm^2. Thus it is suggested that the Mg-preflow in the p-AlGaN EBL plays a decisive role for the declined EQE and increased PW shift of green LEDs at 300 K as well as the reversal in EQE at 100 K.

We surmise that the declined EQE and increased PW shift in sample B at 300 K should be correlated with the mechanism of holes injection into the *c*-plane MQWs. On the one hand, the bandgap of sidewall MQWs in the V-pits is several hundreds of meV higher than that of the *c*-plane MQWs, thus the energy barrier for the lateral transport of carriers is provided to prevent holes from flowing through the V-pits.[11] On the other hand, the voltage applied to the *c*-plane EBL is higher than that of the EBL in the V-pits due to the thicker EBL at the *c*-plane. The voltage difference applied to the *c*-plane and V-pits EBL can promote holes to be conducted by the sidewall MQWs of the V-pits. Hence, it is the competition between energy barrier and the voltage difference that decides the main path

for holes to be injected into the MQWs. Compared with sample A, sample B with higher Mg doping concentration in EBL has lower resistivity, and it causes the smaller voltage difference to be not high enough to compensate the energy barrier, which blocks the holes more effectively to flow via the V-pits.[10] Consequently, holes for sample A are easier to flow through the sidewall of V-pits (path 1), but through the *c*-plane (path 2) for sample B, as shown in Fig. 4. The V-pits are believed to bring holes closer to the QWs near the n-GaN, which are away from the p-GaN.[12] Thus at low current density, the emission position in sample B is closer to the p-GaN compared with sample A. Previous investigations have shown that, the total strain energy stored in the MQWs is accumulated with the increase of QW number due to the mismatch between InGaN wells and GaN barriers, and the strain relaxation occurs in upper QWs closer to p-GaN by the formation of structure defects such as stacking faults, misfit dislocations above the critical strain energy.[13] Therefore, sample B with emission position closer to p-GaN has lower EQE at 300 K despite its higher doping concentration in the EBL. Moreover, the strain relaxation is accompanied by an increase of indium incorporation.[14] Enhanced indium incorporation in QWs closer to p-GaN accounts for the longer PW at low current density for sample B (see Fig. 3(c)). Since there are more QWs for emission due to holes easier to flow through the V-pits in sample A, the larger full-width at half maximum (FWHM) of sample A shown in Fig. 3(d) is observed at low current density.

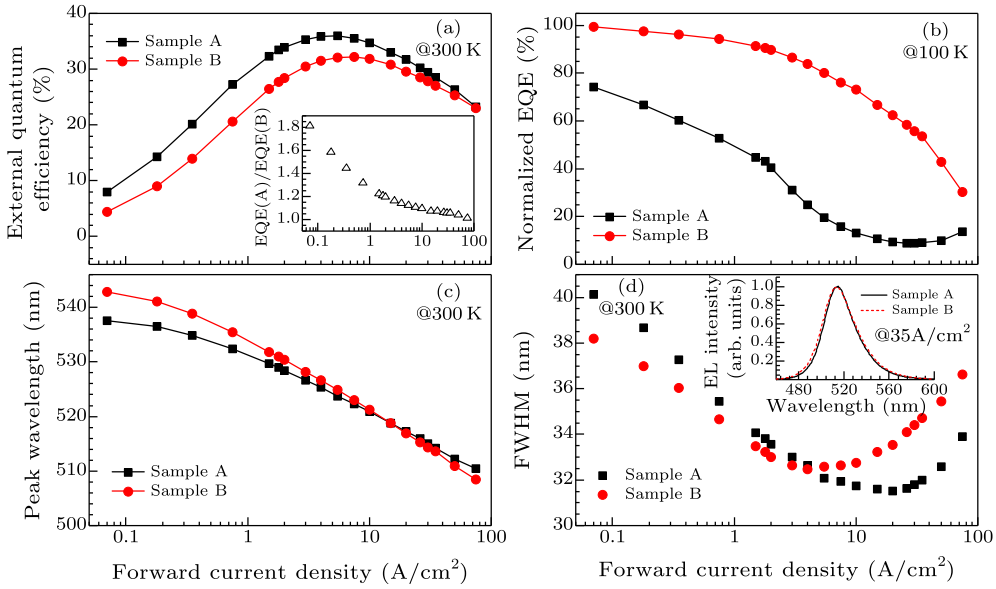

Fig. 3. (a) EQE of samples A and B and EQE ratio of sample A to sample B at 300 K. (b) Normalized EQE of samples A and B at 100 K. (c) The PW of samples A and B at 300 K. (d) The FWHM of samples A and B at 300 K.

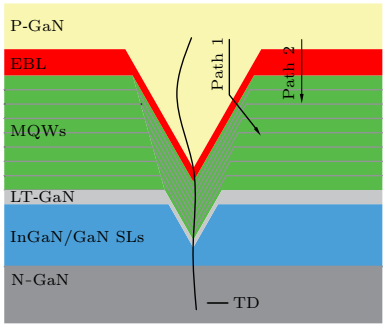

Fig. 4. Schematic diagram of V-pits and the different paths for hole injection into MQWs.

As the current density increases, the voltage applied to the *c*-plane EBL, which is much thicker than that in the V-pits, would increase rapidly, so does the voltage difference. The increased voltage difference would offset the energy barrier of the sidewall MQWs and drive holes to flow through the sidewall of the V-pits, which leads to a larger proportion of holes in sample B injected into MQWs through the V-pits with the current density increasing. As a result, the emission position in sample B would reasonably move towards QWs with less dislocation closer to n-GaN side. Thus the nonradiative recombination rate in sample B is reduced as the injection current rises, which should be responsible for the reduced difference in EQE between the two samples. Moreover, when the injection current in QWs increases, more injected carriers can populate the higher energy levels due to the state-filling effect, then recombine and emit higher energy photons. Due to the higher doping concentration of the EBL region in sample B, the band filling induced blue-shift in sample B is much more sensitive to the increase of current density, thus the shorter PW of sample B is observed when the current density exceeds 15 A/cm^2, as shown in Fig. 3(c). This can be evidenced by the

larger FWHM in sample B at high current density (see Fig. 3(d)). From the inset of Fig. 3(d), the FWHM spread at 35 A/cm^2 in sample B is mainly induced by the high energy side, which also indicates that sample B has higher band-filling level. As for the higher normalized EQE of sample B at 100 K, it can be well accounted for the thermal deactivation of nonradiative recombination centers (NRCs) at low temperature and the higher doping concentration of the EBL.

In addition to the higher normalized EQE in sample B at 100 K, efficiency droop is also well suppressed at cryogenic temperatures in sample B. Figures 5(a) and 5(b) depict the dependence of normalized internal quantum efficiency (IQE) on the current density over a wide range of temperatures (100–350 K). The common improvements in the maximum IQE and the maximum IQE shift to lower current density are observed in both the samples as the temperature drops, which are believed to benefit from the thermal deactivation of NRCs. Moreover, the less obvious efficiency droop for sample B is observed at larger current density compared with that of sample A. The acceptors freeze out due to the high Mg acceptor ionization energy in GaN at cryogenic temperatures, resulting in exacerbated carrier asymmetry in concentration and electron leakage from the MQWs. The hole concentration in p-layer exhibits a strong dependence on doping concentration and the effective activation energy for Mg acceptor decreases with increasing doping concentration.[15] Therefore, one can guess that the less obvious efficiency droop at low temperature in sample B may be caused by its smaller carrier asymmetry.

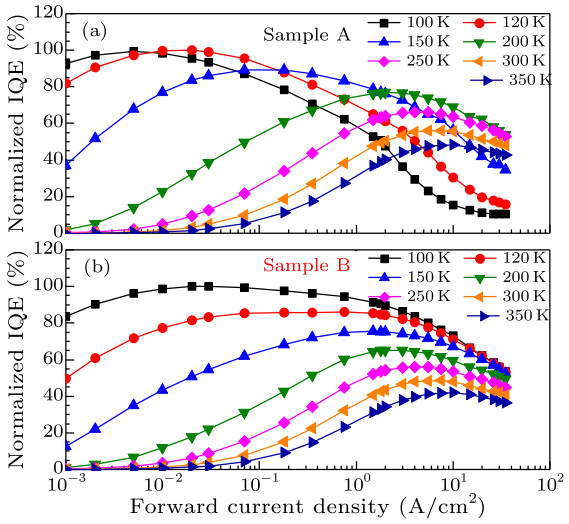

Fig. 5. Measured normalized IQE as a function of forward current density at various temperatures between 100 K and 350 K, plotted in semi-log scale for two samples.

Further evidence for the smaller carrier asymmetry at cryogenic temperatures in sample B can be provided by a careful observation of the EL spectra at 100 K in Fig. 6, drawn in a logarithmic scale. There are two peaks at about 525 nm (P1) and 417 nm (P2), which can be attributed to the quantum well transitions and Mg-related transition, respectively. However, unlike the P2 in sample A appearing at 0.35 A/cm^2, the P2 in sample B emerges at a higher current density of 20 A/cm^2, which indicates the effective suppression of electrons leakage into p-GaN for sample B, and also agrees with the results in Fig. 5. At cryogenic temperatures, the high doping concentration of EBL in sample B results in more thermally activated holes and resultant to smaller carrier asymmetry in electron and hole concentration in the MQWs, which suppresses the electrons overflow into p-layer and then alleviates the efficiency droop. This also well supports the better-normalized EQE at 100 K for sample B.

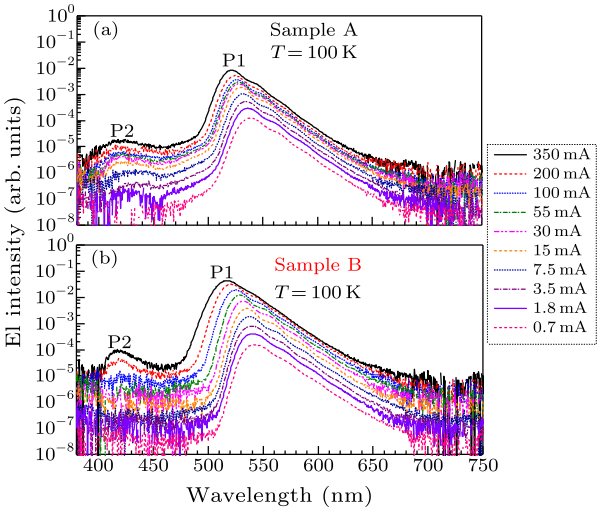

Fig. 6. EL spectra of the two samples at different injection currents at 100 K.

In summary, InGaN/GaN MQWs green LEDs with and without Mg-preflow in p-AlGaN EBL have been studied. The emission efficiency for the sample with Mg-preflow in p-AlGaN EBL reduced at room temperature despite higher Mg-doping concentration in EBL. The position of emission shift towards p-GaN with increasing Mg-doping concentration in EBL, which results in higher nonradiative recombination rate due to accumulated strain relaxation and dislocations, can be responsible for it. Hence, Mg-doping concentration in p-AlGaN EBL for high In content of green LEDs with V-pits, is not as high as possible before it deteriorates the quality of QW. However, when the discrepancy between MQWs disappears, it might be different and needs to be further investigated in the future. Furthermore, the sample with Mg-preflow in EBL can suppress the efficiency droop effectively at cryogenic temperatures due to smaller carrier asymmetry. Consequently, alleviating the carrier asymmetry could be a promising way to improve the efficiency droop at low

temperatures.

References

[1] Guo M, Guo Z Y, Huang J, Liu Y and Yao S Y 2017 *Chin. Phys.* B **26** 028502

[2] Zhao Y K, Li Y F, Huang Y P, Wang H, Su X L, Ding W and Yun F 2015 *Chin. Phys.* B **24** 056806

[3] Meyaard D S, Lin G B, Cho J, Fred Schubert E, Shim H, Ham S H, Kim M H, Sone C and Kim Y S 2013 *Appl. Phys. Lett.* **102** 251114

[4] Zhao Y K, Yun F, Wang S, Feng L G, Su X L, Li Y F, Guo M F, Ding W and Zhang Y 2016 *J. Appl. Phys.* **119** 105703

[5] Zhang Z H, Tan S T, Kyaw Z, Ji Y, Liu W, Ju Z G, Hasanoy N, Sun X W and Demir H V 2013 *Appl. Phys. Lett.* **102** 193508

[6] Zhang Y, Zhang Z H, Tan S T, Hernandez-Martinez P L, Zhu B, Lu S, Kang X J, Sun X W and Demir H V 2017 *Appl. Phys. Lett.* **110** 033506

[7] Mo C L, Fang W Q, Pu Y, Liu H C and Jiang F Y 2005 *J. Cryst. Growth* **285** 312

[8] Liu J, Feng F, Zhou Y et al 2011 *Appl. Phys. Lett.* **99** 111112

[9] Mao Q H, Liu J L, Quan Z J, Wu X M, Zhang M and Jiang F Y 2015 *ECS J. Solid State Sci. Technol.* **4** R44

[10] Tomiya S, Kanitani Y, Tanaka S, Ohkubo T and Hono K 2011 *Appl. Phys. Lett.* **98** 181904

[11] Hangleiter A, Hitzel F, Netzel C, Netzel, Fuhrmann D, Rossow U, Ade G and Hinze P 2005 *Phys. Rev. Lett.* **95** 127402

[12] Li Y F, Yun F, Su X L, Liu S, Ding W and Hou X 2014 *J. Appl. Phys.* **116** 123101

[13] Cho H K, Lee J Y, Kim C S and Yang G M 2002 *J. Appl. Phys.* **91** 1166

[14] Wang H, Jiang D S, Jahn U, Zhu J J, Zhao D G, Liu Z S, Zhang S M, Qiu Y X and Yang H 2010 *Physica* B **405** 4668

[15] Kozodoy P, Xing H, Denbaars S P, Mishra U K, Saxler A, Perrin R, Elhamri S and Mitchel W C 2000 *J. Appl. Phys.* **87** 1832